Mitochondrial and sarcoplasmic reticulum abnormalities in cancer cachexia: Altered energetic efficiency?

Mitochondrial and sarcoplasmic reticulum abnormalities in cancer cachexia: Altered energetic efficiency? / Fontes-Oliveira CC; Busquets S; Toledo M; Penna F; Aylwin MP; Sirisi S; Silva AP; Orpí M; García A; Sette A; Genovese MI; Olivan M; López-Soriano FJ; Argilés JM. - In: BIOCHIMICA ET BIOPHYSICA ACTA-GENERAL SUBJECTS. - ISSN 0304-4165. - STAMPA. - 1830:3(2013), pp. 2770-2778.

DOI:10.1016/j.bbagen.2012.11.009

ABSTRACT

Background: Cachexia is a wasting condition that manifests in several types of cancer, and the main characteristic is the profound loss of muscle mass. **Methods:** The Yoshida AH-130 tumour model has been used and the samples have been analyzed using transmission electronic microscopy, real-time PCR and Western blot techniques. **Results:** Using *in vivo* cancer cachectic model in rats, here we show that skeletal muscle loss is accompanied by fiber morphologic alterations such as mitochondrial disruption, dilatation of sarcoplasmic reticulum and apoptotic nucleus. Analyzing the expression of some factors related to proteolytic and thermogenic processes, we observed in tumor-bearing animals an increased expression of genes involved in proteolysis such as ubiquitin ligases Muscle ring finger 1 (MuRF-1) and Muscle Atrophy F-box protein (MAFBx). Moreover, an overexpression of both sarco/endoplasmic Ca^{2+}-ATPase (SERCA1) and adenine nucleotide translocator (ANT1) (factors related to cellular energetic efficiency) was observed. Tumor burden also leads to a marked decreased in muscle ATP content. **Conclusions:** In addition to muscle proteolysis, other ATP-related pathways may have a key role in muscle wasting, both directly by increasing energetic inefficiency, and indirectly, by affecting the sarcoplasmic reticulum-mitochondrial assembly that is essential for muscle function and homeostasis. **General Significance:** The present study reports, for the first time?, profound morphological changes in cancer cachectic muscle, which are visualized mainly in alterations in sarcoplasmic reticulum and mitochondria. These alterations are linked to pathways that can account for some of energy inefficiency associated with cancer cachexia.

Key Words: Cancer cachexia / muscle wasting / Sarcoplasmic reticulum / Mitochondria / SERCA / ANT1

INTRODUCTION

In advanced malignant diseases, cachexia appears to be one of the most common systemic manifestations. The presence of cachexia always implies a poor prognosis, having a great impact on the patients' quality of life and survival [1]. The skeletal muscle loss is the main characteristic of cancer cachexia and the principal cause of function impairment, fatigue and respiratory complications [2]. Several important molecular mechanisms have been shown to be involved in the increased muscle catabolism observed in cancer-induced cachexia, such as greater ubiquitin-proteasome-dependent proteolysis, apoptosis, and activation of uncoupling proteins [3]. Interaction of these mechanisms leads to muscle-mass loss by promoting protein and DNA breakdown and energy inefficiency.

Skeletal muscle is a very heterogeneous tissue and is used to respond to a broad range of functional demands in each animal species. It represents approximately 50% of the whole total weight and plays a central role in the whole-body metabolism [4]. Consequently, the loss of muscle in catabolic syndromes, such as cancer cachexia, represents a devastating condition not only for patient's quality of life, but also as a surgical risk and also decreasing the response to chemotherapy [3, 5]. It is important to emphasize that approximately 30% of body weight loss represents a 75% of muscle loss. This factor leads to patient death, and it is the most prominent phenotypic feature in cancer cachexia [6]. In many years, the experts are challenging to understand what mechanisms are involved in the maintenance of muscle mass for the development of strategies to attenuate the wasting and improve muscle function [7].

It is known that mitochondria and sarcoplasmic reticulum (SR) have a key role in the muscular function. This advantageous assembly reflects the Ca^{2+} releasing from SR, stimulating mitochondrial ATP production helping to meet increased energy demand during muscle contraction, a process called excitation-contraction (EC) coupling [8]. On the other hand, functionally intact mitochondria inhibit undesired localized SR Ca^{2+} release by controlling the local redox environment of the calcium release units (for a review, see ref. [8]). Thus, bidirectional SR-mitochondrial communication provides a powerful local

control mechanism for integrating Ca^{2+} release/reuptake and ATP utilization during muscle contraction with ATP production and skeletal muscle bioenergetics [9].

Reduced thermodynamic efficiency will result in an increased weight loss. The laws of thermodynamics are silent on the existence of variable thermodynamic efficiency in metabolic processes. Therefore such variability can be related to differences in weight loss. An alteration of energy balance is the immediate cause of cachexia [10]. Although alterations of energy intake are often associated with cachexia, it has lately become clear that increased energy expenditure is the main cause of wasting associated with different types of pathological conditions, such as cancer, infections and chronic heart failure. Different types of molecular mechanisms contribute to involuntary body weight loss [11].

Taking into consideration that skeletal muscle loss is the most prominent characteristic of cancer cachexia, and that the mitochondria and SR have an important role in the muscle function and energetic metabolism [2], the purpose of this work has been to examine if a dysregulation of mitochondria and SR functions could be involved in the development of cancer cachexia in animals bearing cachectic tumors, analyzing the putative pathways involved in energy efficiency and homeostasis.

MATERIAL AND METHODS

Animals

5 weeks old male Wistar rats (Interfauna, Barcelona, Spain) were maintained at 22 ± 2 °C with a regular light-dark cycle (light on from 08:00 a.m. to 08:00 p.m.) and had free access to food and water. The diet (Panlab, Barcelona, Spain) consists of 63.9% carbohydrate, 14.5% protein, and 4% fat (the residue was non-digestible material). Food intake was measured daily. All animal manipulations were conducted in accordance with the European Community guidelines for the use of laboratory animals.

Tumor inoculation

Rats were divided into two groups, namely controls (n=6) and tumor hosts (n=7). The latter received an intraperitoneal inoculum of 10^8 AH-130 Yoshida ascites hepatoma cells obtained from exponential tumors [12]. 8 days after tumor transplantation, the animals were weighed and anesthetized with an i.p. injection of ketamine/xylazine mixture (3:1) (Imalgene and Rompun respectively). The tumor was harvested from the peritoneal cavity, and its volume and cellularity were evaluated. Several tissues were rapidly excised, weighed, and frozen in liquid nitrogen except for the muscles processed for electron microscopy and histology (see below).

Histology, SDH staining and total activity

During rat sacrifice, the EDL muscles were rapidly excised and divided in two parts in the mid-belly region, half directly frozen in liquid nitrogen for the enzymatic activity, half mounted in OCT and frozen in melting isopentane for histology. Ten micrometers of transverse sections were cut on a cryostat and later

stained for SDH (succinate dehydrogenase) incubating for 30 min at 37°C with 1 mg/mL NTB (nitrotetrazolium blue chloride) and 27 mg/mL Na-succinate in PBS. Afterwards the slides were washed three times in PBS, mounted with glycerol and photographed at different magnifications. Fiber cross-sectional area (CSA) was determined on randomly chosen 100 individual fibers (for both oxidative and glycolytic ones) by the Image J software.

As for the total SDH activity, the muscles were homogenized (5% wt/vol) in ice-cold 150 mM NaCl, 10 mM KH_2PO_4, 0,1 mM EGTA, 2 times x 30 sec. using a turrax device and centrifuged 5 min. at 800 x g. The supernant was collected and total protein content measured using the BCA protein assay (Pierce, Thermo Fisher Scientific, Rockford, IL, USA). 50µL of protein homogenate were incubated with 200 µL reaction buffer containing 10 mM Na-succinate, DCPIP 50 µg/mL, 10 mM phosphate buffer (pH 7,4), 2 mM KCN, 10 mM $CaCl_2$, 0,05% BSA. The absorbance at 600 nm was measured at t0, 3 min and 20 min after the addition of proteins. The rate of disappearance of the absorbance between 3 and 20 min was corrected for the total protein loaded and used to calculate the SDH content.

Transmission Electronic Microscopy

Muscle pieces of 1 mm^2 were removed under a stereomicroscope and transferred to glass vials filled with 2% parafomaldehyde and 2.5% glutaraldehyde in phosphate buffer. They kept in the fixative during 24 h at 4ºC. Then, they were washed with the same buffer and potsfixed with 1% osmium tetroxide in the same buffer containing 0.8% potassium ferricyanide at 4ºC. Then the samples were dehydrated in acetone, infiltrated with Epon resin during 2 days, embedded in the same resin orientated for longitudinal sectioning and polymerised at 60ºC during 48 hour. Semithin sections were made in order to look for muscle fibers at light microscope. When they were found, ultrathin sections were obtained using a Leica

Ultracut UC6 ultramicrotome and mounting on Formvar-coated copper grids. They were staining with 2% uranyl acetate in water and lead citrate. Then, sections were observed in a JEM-1010 electron microscope (Jeol, Japan) equipped with a CCD camera SIS Megaview III and the AnalySIS software. Intermyofibrillar mitochondrial morphology was classified into unchanged and altered (swelling-related ultraestructural changes). Mitochondrial counting was performed from 25-30 micrographs, which were fields randomly taken at 20000x magnification, from three different areas of one grid.

ATP measurement

The determination of ATP using bioluminescence was performed using the commercially available kit ATP Bioluminescence Assay Kit CLS II (Roche) according to manufacturer's recommendations. Briefly, GSN muscles were homogenized in PBS (proportion 1:10 w/v). Then, the samples were diluted 10x in 100 mM Tris, 4 mM EDTA (pH 7.75), incubated 2 minutes at 100°C and centrifuged 1 minute at 1000xg. The supernatant was transferred to a new tube. In a multiwell black plate (96 wells - Packard) 50 µL of the sample and 50 µL of the Luciferase reagent were added. The luminescence was measured in a Luminometer at 562 nm with an integration time of 10 seconds. The ATP concentrations were obtained from a log-log plot of the standard curve data.

Real-time PCR (polymerase chain reaction) better at the bottom, respecting the order of the results

Total RNA was extracted by using Tripure Isolation Reagent (Roche Applied Science, Switzerland) according to manufacturer's recommendations. Expression of *SERCA1* (5'- TTG TCC TAT TTC GGG GTG AG-3' and 5'-TCC CAC AGA GAC TTG CCT TC-*3*'), *SERCA2* (5'-GCT TGT CCA TGT CCC TTC AC-3' and 5'-ACT CCA GTA TTG CAG GCT CC-3'), *ANT1* (5'-GCT GGT GTC CTA TCC GTT TG-3' and 5'-CAG TCA AGT GTC CCC GTG TA-3'), *RyR1*(5'-GTC TCT GTC AGT TCG AGC CC-3' and 5'-GCC AAC TTG TCA GTC ATG GA-3'), *MFN2*

(5'-GAG AGG CGA TTT GAG GAG TG-3' and 5'- GTC AAT GAA TCT CAG CCG GT-3'), *CALP1* (5'-GAG GAA GAT GGG TGA GGA CA-3' and 5'- GCT GAG GTG GAT GTT GGT CT-3'), *PGC-1α* (5'-AAG GTC CCC AGG CAG TAG AT-3' and 5'-TCA GAC TCC CGC TTC TCA T-3'), *UB* (5'-CAC CAA GAA GGT CAA ACA GGA-3' and 5'- CAA ACC CAA GAA CAA GCA CA-3'), *MURF* (5'-GTG AAG TTG CCC CCT TAC AA-3' and 5'-GTG GCT GTT TTC CTT GGT CA-3') and *MAFbx* (5'-TGT GCG ATG TTA CCC AAG AA-3' and 5'- GGT GAA AGT GAG ACG GAG CA-3') were confirmed in each correspondent group. Primer sequences were designed through Primer3 software (http://frodo.wi.mit.edu/cgi-bin/primer3/primer3_www.cgi).

The Operon tool (https://www.operon.com/oligos/toolkit.php) was used to check the putative primer-dimer formation. All reactions were performed with Power SyBR® Green Master Mix (Applied Biosystems) according to manufacturer's instructions. The relative amount of transcripts was calculated using comparative C_T method and *Acidic Ribosomal Phosphoprotein P0* mRNA was used for normalization [13].

Western Blot

Protein isolations from EDL and GSN muscles were performed using the Mitochondria Isolation Kit for Rodent (Mitosciences),allowing the separation of total and mitochondrial fractions. 40 µL of a protease inhibitor cocktail (Complete Roche, Stock solution 25x) was added per mL of isolation buffer. Protein concentrations were determined by the method of bicinchoninic acid (Pierce). Equal amounts of proteins (50 µg) were heat denatured in sample loading buffer (50 mmol/L Tris-HCl pH 6.8, 100 mmol/L DTT, 2% SDS, 0.1% bromophenol blue, 10% glycerol). The samples were loaded on a 4-15% Tris-HCl gel (Ready Gel Biorad) and transferred to Immobilon membranes (Immobilon polyvinylidene difluoride, Millipore). The membranes were blocked with 5% PBS-non fat dry milk and then incubated with Anti-SERCA1 (primary antibody; dilution 1:1000 monoclonal anti-mouse; Sigma), Anti-SERCA2 (primary antibody; dilution 1:1000 monoclonal anti-mouse; Sigma), Anti-ANT1 (primary antibody; dilution 1:500

polyclonal anti-goat; Santa Cruz). Anti-Na^+K^+-ATPase alpha subunit (primary; dilution 1:100 monoclonal anti-mouse; Developmental Studies Hybridoma Bank, Iowa) was used for normalization. Anti-goat (dilution 1:5000; Bio Rad) and anti-mouse (dilution 1:10000; Bio Rad) IgG-HRP conjugate were used as secondary antibodies. The membrane-bound immune complexes were detected by an enhanced chemiluminescence system (EZ-ECL, Amersham Biosciences).

Statistical analysis

Statistical analysis of the data was performed by means of one-way analysis of variance (ANOVA).

RESULTS AND DISCUSSION

The implantation of the Yoshida AH-130 ascites hepatoma caused a marked decrease in body weight, together with an important decrease in skeletal muscle mass represented through 27% of extensor digitorius longus (EDL) and 25% of gastrocnemius (GSN) and 24% of tibialis when compared with control animals (Figure 1A; Table S1). These changes were accompanied by a significant decrease in food intake (18%). These data agree with previous results from our own laboratory [12].

A thorough analysis of muscle morphology in EDL cross sections of controls and AH-130 bearing rats shows that muscle atrophy occurs in both fast and slow twitch muscle fibers. In fact, the cross section area is dramatically reduced in both oxidative and glycolytic fibers (SDH positive and negative, respectively; Figure 1C-D). Such result suggests that muscle wasting in tumor-bearing animals is not selective for a fiber type, although previous results support the notion that fast fibers are the most affected in cancer cachexia […]. In order to measure the gross mitochondrial amount, quantitative biochemical assessment of total SDH activity in muscle homogenates was performed. The results show a lower SDH activity (corrected for total protein content; Figure 1 B) in the muscles from AH-130 bearing rats, evidencing a selective reduction of mithochondrial amount and prompting us to deeper investigate the effects of tumor growth on mitochondial morphology and energetics.

Fiber cross-sectional area (CSA) was determined on oxidative and glycolytic fyber types from EDL muscles indicating that in both fiber types atrophy is present (Figure 1C and 1D). The results are indicated as percentage of fiber number of different areas and it could be observed that in tumour-bearing animals there are an increased number of fibers with small area. It is also observed that total SDH activity is lower in EDL from tumour-bearing animals pointing out that there was a damage in the mitochondria of this group.

Tumor burden induced important morphological changes at the level of skeletal muscle. In Figure 2, the EDL micrographs from control animals show organized sarcomeres, with normal mitochondrial morphology (A-F), whereas the micrographs (G-L) from tumor-bearing rats show disorganized myofibers, dilated SR and a significant increase, both in the surface area and number of mitochondria. Total mitochondrial area showed a threefold increase. The presence of lipid inclusions along the muscle fibers can also be observed in the tumor-bearing animals. In relation to changes induced by tumor burden in GSN muscles (Figure 3), and although the total mitochondrial number was decreased, surface area was significantly increased and the total mitochondrial area was increased 2.6 times. There were also important morphological differences. In control group, sarcomeres were organized (Figure 2 A-F); nucleus contained clear nucleolus and a homogeneous nuclear membrane; mitochondria presented clear cristae and aligned with the triad. Conversely, mitochondria from tumor-bearing animals muscles showed a clear disruption of cristae (Figure 3J, 3K, 3L). Cristae were also often whorled (Figure 3J).

Muscle morphology in the tumor-bearing animals also included sarcomere disorganization, nucleus with an irregular membrane and chromatin compaction (Figure 3H, 3I), features that characterize the apoptotic process. Indeed, apoptosis is linked to muscle wasting during cancer, both in animals [14] and human subjects [15]. As can be observed in Figure 2, in addition to a clear mitochondrial damage, the SR is dilated, with profound alterations in the triad structure (Figure 2L). It is interesting to observe that satellite cells show nucleus with apoptotic morphology similar to what is observed in GSN muscle fibers (Figure 3G and I). Previous studies have shown mitochondrial defects associated with the development of myopathies [16, 17]. The results presented here agree with those that link apoptosis with higher mutation rate in mitochondrial genes and an increased mitochondrial mass in human myopathies that are associated with intolerance to exercise, defects in the energy production and muscle weakness [18].

New experiment PAZ: Additionally to the quatification of area and number of mitochondrias, the percentatge of normal and altered mitochondria have been also measured. As can be seen in figure 4, EDL and GSN from tumour-bearing animals showed an increased number of altered mitochondria compared with the control muscles. This result is in accordance to the decreased ATP content (in GSN) and to the decreased SDH activity (in EDL) in tumour-bearing muscles.

Table 1 shows the consequences of tumor burden on pattern of gene expression in both GSN and EDL muscles. It can be seen that tumor-bearing rats manifested a marked increase in expression for genes related to muscle proteolysis such as ubiquitin (*UB*) (by 5.4-fold and 3.4-fold for EDL and GSN, respectively), muscle specific ubiquitin ligases *MuRF-1* (by 3-fold and 5.5-fold for EDL and GSN, respectively) and *MAFBx* (by 6.2-fold and 5.4-fold for EDL and GSN, respectively), and also *calpain-2* (2.2-fold for both muscles). These results agree with previous results from our own group, where it showed that muscle proteolysis is a common mechanism linked to cachexia present in cancer. [12, 19], Recent studies have shown that MAFBx ligase seems to be involved in the direct degradation of MyoD protein and myofibrillar proteins, whereas MuRF-1 seems to be involved in the degradation of thick filaments [20, 21]. Calcium-dependent proteases (calpains) also seem to play a role in the muscle wasting process [22].

SR and mitochondria have an important inter-relationship and the orchestral regulation of share pathways between these organelles is critical for Ca^{2+} signaling in EC coupling, for the maintenance of cellular homeostasis, for energy supply and for cellular fate under stress conditions [8, 9]. Based on the morphological alterations in these organelles found in cancer cachexia, we decide to analyze if the disruption of SR-mitochondrial communication could be an important factor to explain muscle dysfunction and posterior muscle loss in cancer cachexia. By means of real time PCR and Western Blot

techniques, the expression of some targets connected to this hypothesis in EDL and GSN muscles was analyzed.

An increased expression of ryanodine receptor 1 (*RyR1*) gene was observed, as shown in the Table 1. This receptor is located in the terminal SR and provides the primary means of SR Ca^{2+} release during skeletal muscle EC coupling. The increase in myoplasmic Ca^{2+} during a single twitch is due almost exclusively to the Ca^{2+} released from RyR1 channels located in triads [23]. Mutations of this gene, that cause a hyperactivation of RyR1, are implicated in malignant hyperthermia (MH), where a rapid and sustained rise in intracellular Ca^{2+} in muscle occurs, that causes a profound alteration in Ca^{2+} homeostasis, leading to a rise in body temperature and muscle rigidity upon exposure to a fluorinated inhalation anesthetic such as halothane [23]. Moreover, the increase of RyR1 and its dysregulation has been shown in muscle weakness and fatigue in aging [24, 25]. Therefore, it can be speculated that overexpression of RyR1 can increase the Ca^{2+} leak from SR in cachexia and can be involved in the stress responses, that triggers proteolytic and apoptotic processes [23, 25].

It is particularly interesting to remark on the significant increased expression in both *SERCA1* and *2* genes in EDL muscles in the tumor-bearing animals, as shown in Table 1. In GSN muscles, tumor burden also resulted in an increased *SERCA1* gene expression by 3.6-fold (Table 1). The sarco/endoplasmic Ca^{2+}-ATPase is a membrane protein abundantly present in skeletal muscles where it functions as an indispensable component of the EC coupling, being at the expense of ATP hydrolysis involved in Ca^{2+} exchange with a high thermodynamic efficiency across the SR membrane [26, 27]. In skeletal muscle, SERCA1 has the capacity to interconvert different forms of energy. Thus, SERCA1 activity may be coupled to Ca^{2+} translocation from the cytosol to the SR, a process that requires a considerable amount of energy, since it represents a dynamic process against a concentration gradient. Some of the energy associated with the activity of the pump is released as heat [28]. Interestingly, the pump may also function in an uncoupled way, releasing just heat without translocating Ca^{2+} [26, 29]. In fact, the rate of uncoupled

ATPase activity is much higher than the coupled one. It is for this reason that SERCA1, in addition to being involved in Ca^{2+} translocation, has also been related to non-shivering thermogenesis [30]. Conversely, in SERCA2 most of the hydrolytic ATP-derived energy is coupled to Ca^{2+} transport to the lumen of the SR [28]. It is clear that in adult mammals, despite a small heat production in brown adipose tissue, the major contributor for thermogenesis is the skeletal muscle since it represents about 50% body weight. The increased gene expression of *SERCA1* was accompanied by increased protein content both in EDL (by 4-fold, Figure 3A) and GSN (by 3.6-fold, Figure 3A) muscles from tumor animals. SERCA2 protein content was also increased in EDL muscles (Figure 3C). It may thus be suggested that SERCA, in particular SERCA1, could be involved in the energetic inefficiency that characterizes the cachectic condition [10]. In fact, upregulation of SERCA1 in skeletal muscle has been described in disuse atrophy [31]. It is also very interesting to remark that ATP consumption by SERCA pumps accounts for 50% of resting metabolic rate in mice [32]. If we take into consideration the fact that cancer patients have an increased energy expenditure [33], which contributes to weight loss, it becomes clear the importance that SERCA pumps may have in cancer cachexia. In addition, previous studies have shown that an increased cytosolic ADP concentration, due to an increased SERCA activity, leads to Ca^{2+} leakage from the SR in fast-twitch muscles, effectively reducing the capacity of SERCA to maintain an adequate Ca^{2+} intracellular gradient, and thus leading to increased energetic inefficiency [34].

It is interesting to note that, in addition to the energetic implications of SERCA, it may play a key role in apoptosis. From this point of view, it was characterized a truncated variant of the SERCA1, S1T, that amplifies ER stress, determines endoplasmic reticulum Ca^{2+} depletion due to increased Ca^{2+} leak, an increased number of endoplasmic reticulum-mitochondria contact sites, and inhibition of mitochondria movements that leads to trigger apoptotic processes [35]. Considering the present morphological results that show the apoptotic processes in cachectic muscles and also previous studies [14], the altered SR-mitochondria interactions could be involved in muscle dysfunction and cell death observed in cachexia.

In the mitochondrial internal membrane, the adenine nucleotide translocator (ANT) carries out the ATP/ADP exchange between cytoplasm and mitochondrial matrix. Interestingly, there are four different ANT isoforms (ANT1, ANT2, ANT3 and ANT4) but ANT1 is the predominant isoform present in skeletal muscle and, although not normally included as a part of the OXPHOS system, it is a key protein regulating the mitochondrial ATP/ADP flux [36]. It seems that the activity of the transporter may be intimately linked to uncoupling of the respiratory chain, basically due to proton leakage across the inner mitochondrial membrane and, therefore, disruption of the electrochemical proton gradient that drives ATP synthesis in the mitochondria [37]. Interestingly, our results show an increased *ANT1* gene expression in both GSN and EDL muscles during tumor growth (2.2 and 2-fold respectively), as shown in Table 1. These increases in mRNA content are accompanied by significant elevations in protein content (Figure 3D, E). These alterations may be an indication of uncoupling in mitochondria from tumor-bearing animals. ANT1 also seems to play a key role in the pathogenesis of fascioscapulohumeral muscular dystrophy, one of the most common hereditary muscle diseases, where ANT1 is significantly elevated in muscle resulting in mitochondrial dysfunction associated with oxidative stress, leading to progressive weakness involving the face, shoulders, hips and feet [38]. In addition, [39] have reported an increased expression of *ANT1* in soleus muscles undergoing immobilization-induced atrophy. Based on above evidences, the high expression of ANT1 in cachexia can be linked to an improved proton leak that leads to a decrease of ATP production, maybe at the beginning of the cachectic stage. In addition to its role in wasting, there is a connection between ANT1 and apoptosis. ANT1 has been known to be a major component of the permeability transition pore complex (PTP), a high conductance channel that cause an abrupt increase in the permeability of small solutes across the inner mitochondrial membrane, contributing to mitochondria-mediated apoptosis [40]. In any case, ANT1 could therefore have an important role in muscle apoptosis during tumor burden [14, 15].

The consequences of the abnormal SR-mitochondrial morphology and molecular profile of expression observed in cachectic muscle were reflected in total muscle ATP content. Indeed, as can be seen in Figure 3F, it was significantly reduced by 17% in the tumor-bearing animals. This could be explained taking into consideration an impairment of oxidative capacity of mitochondria, leading to PTP formation and apoptotic signals. Similar observations have previously been reported [41]. In fact, very recently, a defect in ATP synthesis during cancer has been described by our group, directly linked to mitochondrial dysfunction [42].

It is worth mentioning the increased gene expression of mitofusin-2 (*Mfn2)* and proliferator-activated receptor gamma coactivator (*PGC-1α*) in EDL muscles of tumor-bearing rats (Table 1). Mfn2 is a mitochondrial protein involved in the regulation of mitochondrial morphology and distribution [43]. Moreover, Mfn2 is related to the interactions between endoplasmic reticulum and mitochondria which govern interorganellar Ca^{2+} signaling, having a key role in endoplasmic reticulum morphology [44]. Moreover, the SR-mitochondrial apposition performed by Mfn2 predisposes mitochondria to high Ca^{2+} microdomains and to the consequent overloading, leading eventually to apoptosis by excessive Ca^{2+} transfer [45, 46]. Furthermore, it is known that PGC-1α participates in the stimulation of Mfn2 expression under a variety of conditions characterized by enhanced energy expenditure (for review, see ref. [47]). Hence, in cachexia the overexpression of *PGC-1α* can activate *Mfn2* expression, this leading to a Ca^{2+} dysregulation and formation of permeability transition pore (PTP), which is involved in apoptotic processes. It is known that *Bax*, a proapoptotic gene, is overexpressed in cachectic muscles [48]; therefore the apoptotic signals in cachexia could also be started by Mfn2 and Bax.

Finally, considering that SERCA and ANT1 are related to energy dissipation in SR and mitochondria, it may be suggest that they could have a role in energy inefficiency associated with cachexia. This process could induce SR stress by high and constant citoplasmic Ca^{2+} levels, having dramatic consequences for the muscle cell, thus leading to a self-amplifying circuitry between SR and

mitochondria by Mfn2 that eventually results in muscle death. The increased Ca^{2+} levels induce a decrease in ATP content not only by OXPHOS dysfunction, but also through thermogenic processes, such as those performed through ANT1. Recent evidences describes SERCA not only as a heat pump, functioning like a thermogenic device in the skeletal muscle, but also as a directly regulator of Ca^{2+} signaling in mitochondria [49, 50]. These facts lead to suggest that the main energy dissipation observed in cachexia could be related to an increased expression of SERCA, more precisely by implication of SERCA reactions that produce heat and also lead to Ca^{2+} leak. The proton leak activity of UCP3 [51] and ANT1 into mitochondria can worsen the catabolic condition in cachexia, potentiate the ADP accumulation [34], Ca^{2+} leak and heat production as represented in the Figure 4. The constant Ca^{2+} leakage from SR and disruption of mitochondrial functions amplify subsequently the degradation signals, triggering proteolytic processes through calpain, cathepsins and Ub-Proteasome systems, and apoptotic signals performed by PTP formation through ANT1 and Bax [48].

CONCLUSIONS

The present study reports, for the first time, profound morphological changes in cancer cachectic muscle, which are visualized mainly in alterations in SR and mitochondria. posar alguna cosa més de morfologia de ME !!!!

These alterations are linked to pathways that can account for some of energy inefficiency associated with cancer cachexia. It is known that SR-mitochondrial assembly is crucial for muscle activity, where SR Ca^{2+} release stimulates the mitochondrial ATP production to supply the increased energy demand during EC coupling [9]. EC uncoupling is a term used to describe a highly reproducible and specific phenomenon, in which the normal EC process in a skeletal muscle fiber is disrupted [52]. This phenomenon is thought to be implicated in situations such as ageing, muscle fatigue and some muscle diseases [52, 53]. Altogether, the present data suggests that EC uncoupling could be an event previous to activation of proteolytic processes in catabolic conditions. Indeed, the factors implicated in EC uncoupling are strictly related to SR and mitochondrial disruption. This condition can activate proteolytic and apoptotic signals, leading to muscle atrophy in cachexia. The therapeutic implications of understanding the commented assembly and the energy dissipation pathways involved, such as SERCA and ANT1 are very obvious and deserve future research and could well lead to new approaches for the treatment of cancer cachexia.

ACKNOWLEDGEMENTS

This work was supported by Ministerio de Ciencia y Tecnología (SAF-02284-2008) grant. Cibely C. Fontes-Oliveira was supported by the Programme Alban (European Union Programme of High Level Scholarships for Latin America, scholarship no. E05D059293BR).

REFERENCES

[1] W.J. Evans, J.E. Morley, J. Argiles, C. Bales, V. Baracos, D. Guttridge, A. Jatoi, K. Kalantar-Zadeh, H. Lochs, G. Mantovani, D. Marks, W.E. Mitch, M. Muscaritoli, A. Najand, P. Ponikowski, F. Rossi Fanelli, M. Schambelan, A. Schols, M. Schuster, D. Thomas, R. Wolfe, S.D. Anker, Cachexia: a new definition, Clin Nutr 27 (2008) 793-799.

[2] M. Bossola, F. Pacelli, A. Tortorelli, F. Rosa, G.B. Doglietto, Skeletal muscle in cancer cachexia: the ideal target of drug therapy, Curr Cancer Drug Targets 8 (2008) 285-298.

[3] J.M. Argiles, R. Moore-Carrasco, G. Fuster, S. Busquets, F.J. Lopez-Soriano, Cancer cachexia: the molecular mechanisms, Int J Biochem Cell Biol 35 (2003) 405-409.

[4] R. Bassel-Duby, E.N. Olson, Signaling pathways in skeletal muscle remodeling, Annu Rev Biochem 75 (2006) 19-37.

[5] E. Bruera, Pharmacological treatment of cachexia: any progress?, Support Care Cancer 6 (1998) 109-113.

[6] M. Muscaritoli, M. Bossola, Z. Aversa, R. Bellantone, F. Rossi Fanelli, Prevention and treatment of cancer cachexia: new insights into an old problem, Eur J Cancer 42 (2006) 31-41.

[7] A. Saini, S. Faulkner, N. Al-Shanti, C. Stewart, Powerful signals for weak muscles, Ageing Res Rev 8 (2009) 251-267.

[8] R.T. Dirksen, Sarcoplasmic reticulum-mitochondrial through-space coupling in skeletal muscle, Appl Physiol Nutr Metab 34 (2009) 389-395.

[9] A.E. Rossi, S. Boncompagni, R.T. Dirksen, Sarcoplasmic reticulum-mitochondrial symbiosis: bidirectional signaling in skeletal muscle, Exerc Sport Sci Rev 37 (2009) 29-35.

[10] J.M. Argiles, B. Alvarez, F.J. Lopez-Soriano, The metabolic basis of cancer cachexia, Med Res Rev 17 (1997) 477-498.

[11] M.J. Tisdale, Mechanisms of cancer cachexia, Physiol Rev 89 (2009) 381-410.

[12] S. Busquets, M.T. Figueras, G. Fuster, V. Almendro, R. Moore-Carrasco, E. Ametller, J.M. Argiles, F.J. Lopez-Soriano, Anticachectic effects of formoterol: a drug for potential treatment of muscle wasting, Cancer Res 64 (2004) 6725-6731.

[13] R. Akamine, T. Yamamoto, M. Watanabe, N. Yamazaki, M. Kataoka, M. Ishikawa, T. Ooie, Y. Baba, Y. Shinohara, Usefulness of the 5' region of the cDNA encoding acidic ribosomal phosphoprotein P0 conserved among rats, mice, and humans as a standard probe for gene expression analysis in different tissues and animal species, J Biochem Biophys Methods 70 (2007) 481-486.

[14] M. van Royen, N. Carbo, S. Busquets, B. Alvarez, L.S. Quinn, F.J. Lopez-Soriano, J.M. Argiles, DNA fragmentation occurs in skeletal muscle during tumor growth: A link with cancer cachexia?, Biochem Biophys Res Commun 270 (2000) 533-537.

[15] S. Busquets, C. Deans, M. Figueras, R. Moore-Carrasco, F.J. Lopez-Soriano, K.C. Fearon, J.M. Argiles, Apoptosis is present in skeletal muscle of cachectic gastro-intestinal cancer patients, Clin Nutr 26 (2007) 614-618.

[16] P. Bernardi, P. Bonaldo, Dysfunction of mitochondria and sarcoplasmic reticulum in the pathogenesis of collagen VI muscular dystrophies, Ann N Y Acad Sci 1147 (2008) 303-311.

[17] W.A. Irwin, N. Bergamin, P. Sabatelli, C. Reggiani, A. Megighian, L. Merlini, P. Braghetta, M. Columbaro, D. Volpin, G.M. Bressan, P. Bernardi, P. Bonaldo, Mitochondrial dysfunction and apoptosis in myopathic mice with collagen VI deficiency, Nat Genet 35 (2003) 367-371.

[18] K. Aure, G. Fayet, J.P. Leroy, E. Lacene, N.B. Romero, A. Lombes, Apoptosis in mitochondrial myopathies is linked to mitochondrial proliferation, Brain 129 (2006) 1249-1259.

[19] M. Llovera, C. Garcia-Martinez, N. Agell, F.J. Lopez-Soriano, J.M. Argiles, Muscle wasting associated with cancer cachexia is linked to an important activation of the ATP-dependent ubiquitin-mediated proteolysis, Int J Cancer 61 (1995) 138-141.

[20] J. Lagirand-Cantaloube, K. Cornille, A. Csibi, S. Batonnet-Pichon, M.P. Leibovitch, S.A. Leibovitch, Inhibition of atrogin-1/MAFbx mediated MyoD proteolysis prevents skeletal muscle atrophy in vivo, PLoS One 4 (2009) e4973.

[21] S. Cohen, J.J. Brault, S.P. Gygi, D.J. Glass, D.M. Valenzuela, C. Gartner, E. Latres, A.L. Goldberg, During muscle atrophy, thick, but not thin, filament components are degraded by MuRF1-dependent ubiquitylation, J Cell Biol 185 (2009) 1083-1095.

[22] P. Costelli, P. Reffo, F. Penna, R. Autelli, G. Bonelli, F.M. Baccino, Ca(2+)-dependent proteolysis in muscle wasting, Int J Biochem Cell Biol 37 (2005) 2134-2146.

[23] A.M. Bellinger, M. Mongillo, A.R. Marks, Stressed out: the skeletal muscle ryanodine receptor as a target of stress, J Clin Invest 118 (2008) 445-453.

[24] O. Delbono, K.S. O'Rourke, W.H. Ettinger, Excitation-calcium release uncoupling in aged single human skeletal muscle fibers, J Membr Biol 148 (1995) 211-222.

[25] J. Aydin, D.C. Andersson, S.L. Hanninen, A. Wredenberg, P. Tavi, C.B. Park, N.G. Larsson, J.D. Bruton, H. Westerblad, Increased mitochondrial Ca2+ and decreased sarcoplasmic reticulum Ca2+ in mitochondrial myopathy, Hum Mol Genet 18 (2009) 278-288.

[26] L. de Meis, A.L. Vianna, Energy interconversion by the Ca2+-dependent ATPase of the sarcoplasmic reticulum, Annu Rev Biochem 48 (1979) 275-292.

[27] M. Periasamy, A. Kalyanasundaram, SERCA pump isoforms: their role in calcium transport and disease, Muscle Nerve 35 (2007) 430-442.

[28] A.P. Arruda, L.A. Ketzer, M. Nigro, A. Galina, D.P. Carvalho, L. de Meis, Cold tolerance in hypothyroid rabbits: role of skeletal muscle mitochondria and sarcoplasmic reticulum Ca2+ ATPase isoform 1 heat production, Endocrinology 149 (2008) 6262-6271.

[29] L. de Meis, ATP synthesis and heat production during Ca(2+) efflux by sarcoplasmic reticulum Ca(2+)-ATPase, Biochem Biophys Res Commun 276 (2000) 35-39.

[30] S. Kjelstrup, D. Barragan, D. Bedeaux, Coefficients for active transport and thermogenesis of Ca2+-ATPase isoforms, Biophys J 96 (2009) 4376-4386.

[31] E.J. Stevenson, P.G. Giresi, A. Koncarevic, S.C. Kandarian, Global analysis of gene expression patterns during disuse atrophy in rat skeletal muscle, J Physiol 551 (2003) 33-48.

[32] S.M. Norris, E. Bombardier, I.C. Smith, C. Vigna, A.R. Tupling, ATP consumption by sarcoplasmic reticulum Ca2+ pumps accounts for 50% of resting metabolic rate in mouse fast and slow twitch skeletal muscle, Am J Physiol Cell Physiol 298 (2010) C521-529.

[33] D.X. Cao, G.H. Wu, B. Zhang, Y.J. Quan, J. Wei, H. Jin, Y. Jiang, Z.A. Yang, Resting energy expenditure and body composition in patients with newly detected cancer, Clin Nutr 29 (2010) 72-77.

[34] W.A. Macdonald, D.G. Stephenson, Effects of ADP on sarcoplasmic reticulum function in mechanically skinned skeletal muscle fibres of the rat, J Physiol 532 (2001) 499-508.

[35] M. Chami, B. Oules, G. Szabadkai, R. Tacine, R. Rizzuto, P. Paterlini-Brechot, Role of SERCA1 truncated isoform in the proapoptotic calcium transfer from ER to mitochondria during ER stress, Mol Cell 32 (2008) 641-651.

[36] M. Klingenberg, The ADP and ATP transport in mitochondria and its carrier, Biochim Biophys Acta 1778 (2008) 1978-2021.

[37] M. Arvier, L. Lagoutte, G. Johnson, J.F. Dumas, B. Sion, G. Grizard, Y. Malthiery, G. Simard, P. Ritz, Adenine nucleotide translocator promotes oxidative phosphorylation and mild uncoupling in mitochondria after dexamethasone treatment, Am J Physiol Endocrinol Metab 293 (2007) E1320-1324.

[38] D. Laoudj-Chenivesse, G. Carnac, C. Bisbal, G. Hugon, S. Bouillot, C. Desnuelle, Y. Vassetzky, A. Fernandez, Increased levels of adenine nucleotide translocator 1 protein and response to oxidative stress are early events in facioscapulohumeral muscular dystrophy muscle, J Mol Med 83 (2005) 216-224.

[39] J.W. Kim, O.Y. Kwon, M.H. Kim, Differentially expressed genes and morphological changes during lengthened immobilization in rat soleus muscle, Differentiation 75 (2007) 147-157.

[40] B. Zhivotovsky, L. Galluzzi, O. Kepp, G. Kroemer, Adenine nucleotide translocase: a component of the phylogenetically conserved cell death machinery, Cell Death Differ 16 (2009) 1419-1425.

[41] J.M. Argiles, F.J. Lopez-Soriano, The energy state of tumor-bearing rats, J Biol Chem 266 (1991) 2978-2982.

[42] C. Constantinou, C.C. Fontes de Oliveira, D. Mintzopoulos, S. Busquets, J. He, M. Kesarwani, M. Mindrinos, L.G. Rahme, J.M. Argiles, A.A. Tzika, Nuclear magnetic resonance in conjunction with functional genomics suggests mitochondrial dysfunction in a murine model of cancer cachexia, Int J Mol Med 27 (2010) 15-24.

[43] D. Bach, S. Pich, F.X. Soriano, N. Vega, B. Baumgartner, J. Oriola, J.R. Daugaard, J. Lloberas, M. Camps, J.R. Zierath, R. Rabasa-Lhoret, H. Wallberg-Henriksson, M. Laville, M. Palacin, H. Vidal, F. Rivera, M. Brand, A. Zorzano, Mitofusin-2 determines mitochondrial network architecture and mitochondrial metabolism. A novel regulatory mechanism altered in obesity, J Biol Chem 278 (2003) 17190-17197.

[44] O.M. de Brito, L. Scorrano, Mitofusin 2 tethers endoplasmic reticulum to mitochondria, Nature 456 (2008) 605-610.

[45] P. Huang, T. Yu, Y. Yoon, Mitochondrial clustering induced by overexpression of the mitochondrial fusion protein Mfn2 causes mitochondrial dysfunction and cell death, Eur J Cell Biol 86 (2007) 289-302.

[46] R. Rizzuto, S. Marchi, M. Bonora, P. Aguiari, A. Bononi, D. De Stefani, C. Giorgi, S. Leo, A. Rimessi, R. Siviero, E. Zecchini, P. Pinton, Ca(2+) transfer from the ER to mitochondria: when, how and why, Biochim Biophys Acta 1787 (2009) 1342-1351.

[47] A. Zorzano, Regulation of mitofusin-2 expression in skeletal muscle, Appl Physiol Nutr Metab 34 (2009) 433-439.

[48] M. Figueras, S. Busquets, N. Carbo, E. Barreiro, V. Almendro, J.M. Argiles, F.J. Lopez-Soriano, Interleukin-15 is able to suppress the increased DNA fragmentation associated with muscle wasting in tumour-bearing rats, FEBS Lett 569 (2004) 201-206.

[49] S. Kjelstrup, L. de Meis, D. Bedeaux, J.M. Simon, Is the Ca2+-ATPase from sarcoplasmic reticulum also a heat pump?, Eur Biophys J 38 (2008) 59-67.

[50] L. de Meis, L.A. Ketzer, R.M. da Costa, I.R. de Andrade, M. Benchimol, Fusion of the endoplasmic reticulum and mitochondrial outer membrane in rats brown adipose tissue: activation of thermogenesis by Ca2+, PLoS One 5 (2010) e9439.

[51] S. Busquets, D. Sanchis, B. Alvarez, D. Ricquier, F.J. Lopez-Soriano, J.M. Argiles, In the rat, tumor necrosis factor alpha administration results in an increase in both UCP2 and UCP3 mRNAs in skeletal muscle: a possible mechanism for cytokine-induced thermogenesis?, FEBS Lett 440 (1998) 348-350.

[52] G.D. Lamb, Mechanisms of excitation-contraction uncoupling relevant to activity-induced muscle fatigue, Appl Physiol Nutr Metab 34 (2009) 368-372.

[53] J.C. Calderon-Velez, L.C. Figueroa-Gordon, [Excitation-contraction coupling in skeletal muscle: questions remaining after 50 years of research], Biomedica 29 (2009) 140-160.

FIGURE LEGENDS

Figure 1

A: EDL muscle weight from control (C) and tumor-bearing (AH-130) rats. B: graph showing the reduction of total SDH activity in AH-130 vs C rats. C: micrographs (4x and 20x magnification) of EDL cross sections stained for SDH activity. Scale bar: 200 μm. D: fiber CSA independently measured in oxidative and glycolytic fibers. Statistical significances were analyzed using one-way ANOVA (* $p<0.05$; *** $p<0.001$).

Figure 2

Electron micrographs depicting morphological mitochondrial differences between extensor digitorum longus (EDL) muscles from control and tumor-bearing rats.

A-F: EDL from control rats. G-L: EDL from tumor-bearing rats. Scale bar: indicated. Graphs are showing differences in intermyofibrilar mitochondria's area and number between control and tumor groups. Mitochondrial counting was performed from 25-30 micrographs, which were fields randomly taken at 20000x magnification, from three different areas of one grid. Statistical significances were analyzed using one-way *ANOVA* (*** $p<0.001$).

Figure 3

Electron micrographs depicting morphological mitochondrial differences between gastrocnemius (GSN) muscles from control and tumor-bearing rats.

A-F: GSN from control rats. G-L: GSN from tumor-bearing rats. Scale bar: indicated. Graphs are showing differences in intermyofibrilar mitochondria´s area and number between control and tumor groups. Mitochondrial counting was performed from 25-30 micrographs, which were fields randomly taken at 20000x magnification, from three different areas of one grid. Statistical significances were analyzed using one-way *ANOVA* (* $p<0.05$; *** $p<0.001$).

Figure 4

Ultraestructural changes in mitochondrial morphology in gastrocnemius and EDL muscles from control and tumor-bearing rats.

A. Pictures A-B: EDL muscle; and C-D: Gastrocnemius muscle. A,C: Control. B,D: Tumor. White arrows are pointing to swelling mitochondrias. Magnification 20000x.

B. Percentage of unchanged and altered (including electro-lucent and swelling alterations) mitochondrias. Statistical significance of the results was determined using one-way ANOVA (* $p<0.05$; ** $p<0.01$).

Figure 5

A, SERCA1 protein content in extensor digitorum longus (EDL) muscles. B, SERCA1 protein content in gastrocnemius (GSN) muscles from control and tumor-bearing rats. C, SERCA2 protein content in extensor digitorum longus (EDL) muscles. D, ANT1 protein content in EDL muscles. E, ANT1 protein content in GSN muscles from control and tumor-bearing rats. Na^+, K^+-ATPase alpha subunit was used as invariant control. F, Differences of ATP content in GSN muscle between control and tumor-bearing rats. Results are expressed as µM ATP/g of GSN muscle. For further details, see Materials and Methods. Columns, mean of four animals in each group; bars, SE. The results are expressed as a percentage of controls. Statistical significances were analyzed using one-way *ANOVA* (* $p<0.05$; ** $p<0.01$).

Figure 6

Hypothetical involvement of sarcoplasmic reticulum and mitochondria alterations in energy inefficiency and muscle wasting during cancer cachexia. SERCA, sarco/endoplasmic reticulum Ca2+-ATPase. ANT1, adenine nucleotide translocator. MFN2: mitofusin 2. PTP, permeability transition pore. ATP, adenosine

triphosphate. EC uncoupling, excitation contraction coupling. OXPHOS: Oxidative phosphorilation system. Ca^{2+}, calcium. ADP, adenosine diphosphate. Pi, inorganic phosphate.

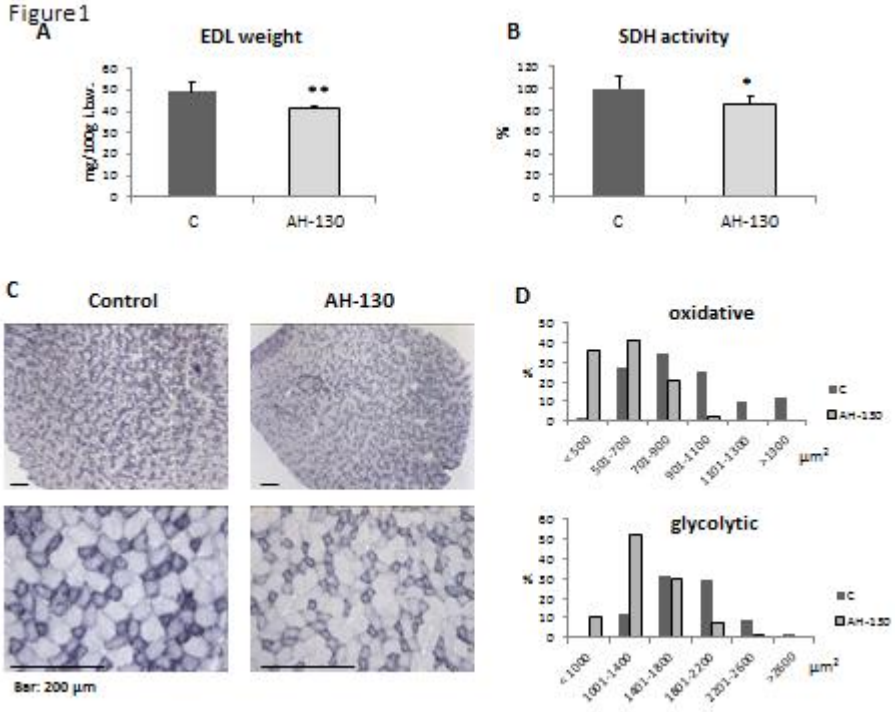

Figure 2

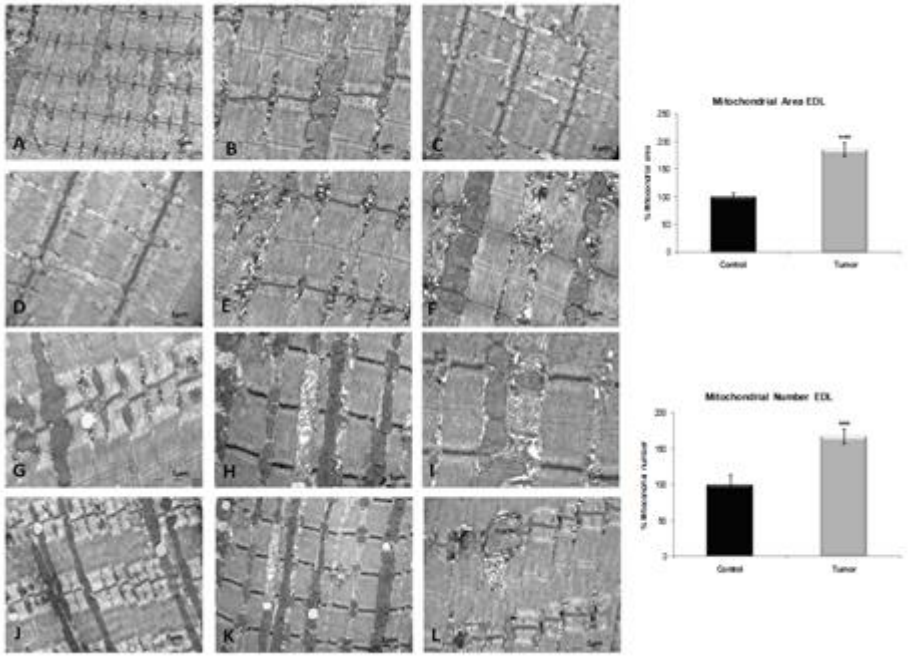

Figure 3

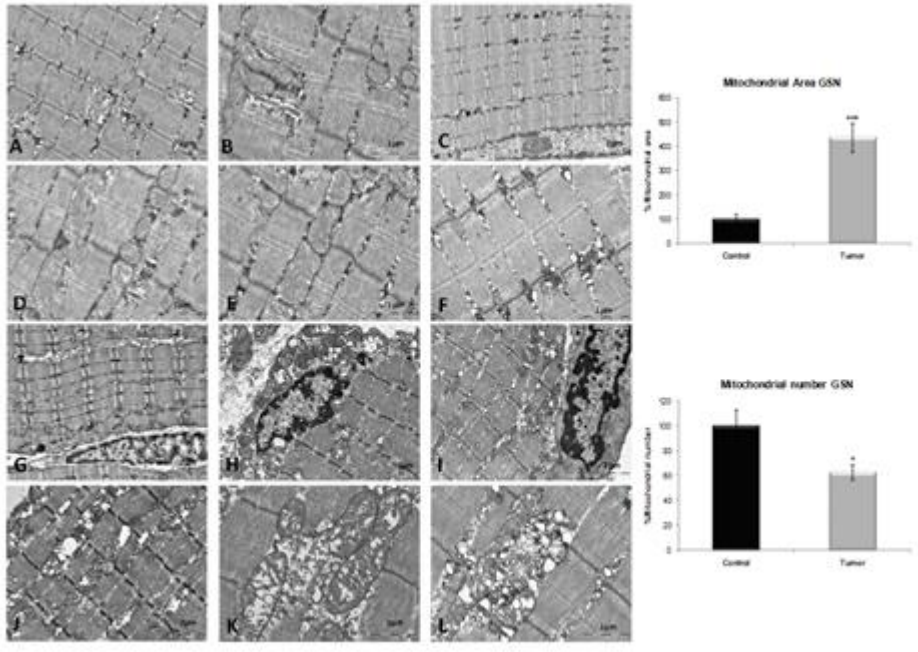

Figure4

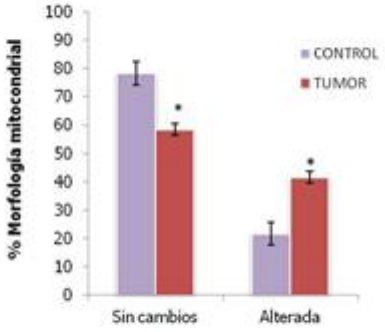

Figure5

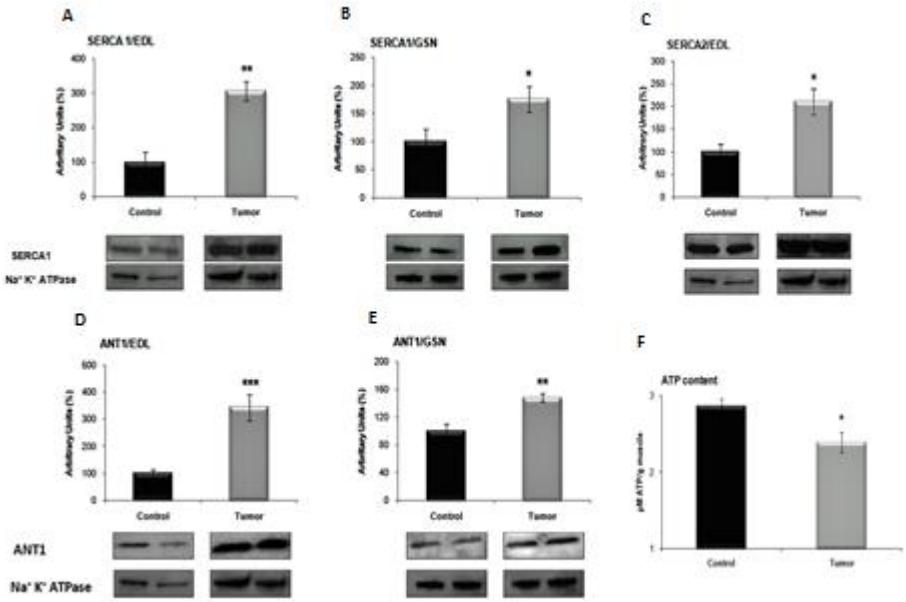

Figure 6

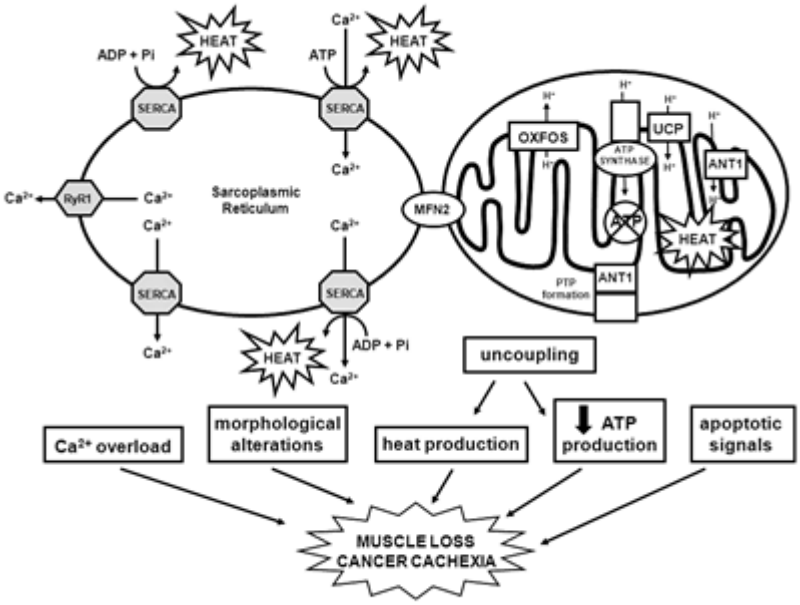
ADP + Pi
HEAT
ATP
HEAT
SERCA
SERCA
Ca2+
Ca2+
RyR1
Ca2+
Sarcoplasmic Reticulum
MFN2
Ca2+
Ca2+
SERCA
SERCA
Ca2+
HEAT
ADP + Pi
Ca2+
H+
OXFOS
H+
H+
UCP
H+
ATP SYNTHASE
H+
ANT1
ATP
HEAT
PTP formation
ANT1
uncoupling
Ca2+ overload
morphological alterations
heat production
ATP production
apoptotic signals
MUSCLE LOSS
CANCER CACHEXIA